Available online at www.sciencedirect.com
SCIENCE DIRECT®
Biochemical Pharmacology 66 (2003) 859–866
Biochemical Pharmacology
www.elsevier.com/locate/biochempharm

P-selectin as a candidate target in atherosclerosis

Tom J.M. Molenaar[1], Jaap Twisk[1], Sonja A.M. de Haas, Niels Peterse, Bram J.C.P. Vogelaar, Steven H. van Leeuwen, Ingrid N. Michon, Theo J.C. van Berkel, Johan Kuiper, Erik A.L. Biessen*

Division of Biopharmaceutics, Leiden/Amsterdam Center for Drug Research, Leiden University, P.O. Box 9502, 2300 RA Leiden, The Netherlands

Received 28 February 2003; accepted 18 May 2003

Abstract

P-selectin is of critical importance in early atherogenesis by initiating leukocyte rolling at the site of endothelial injury. In order to validate P-selectin as a candidate target for the development of anti-atherogenic strategies, we wanted to obtain quantitative information on P-selectin expression, and identify novel peptide-based lead structures that interact with P-selectin. P-selectin mRNA expression in the aortic arch and in other tissues of apoE-deficient (apoE−/−) mice was determined by real-time PCR technology. P-selectin mRNA expression of apoE−/− mice increased steadily with age to levels 14-fold higher than that of control animals. The onset and level of P-selectin expression correlated well with the extent of lesion development, and was more specific for atherosclerotic tissue as compared with other adhesion molecules. Phage display technology was used to obtain novel P-selectin antagonists. Phage display selections resulted in the isolation of a highly P-selectin-specific phage clone. Synthetic peptide-equivalents of this clone displaced the binding of the parent phage and antagonized the binding of a sialyl Lewis^x analogue to P-selectin. In conclusion, P-selectin expression correlates with early and advanced atherosclerotic lesion development. P-selectin ligands, like the lead structure we have developed here, can therefore be considered as promising tools to identify, target or antagonize P-selectin function within the chronically inflamed arterial wall.

Keywords: Antagonists; Atherosclerosis; Endothelial receptors; Gene expression; Inflammation; P-selectin

1. Introduction

The pathogenesis of atherosclerosis contains an important inflammatory component. Early lesion development involves the adhesion of leukocytes, particularly monocytes, to the vascular endothelium at sites of injury. After migration into lesion-prone areas of the arterial vasculature, monocytes ingest lipids to become foam cells, which is a hallmark of atherosclerotic plaque formation [1].

Leukocyte extravasation occurs in several steps, regulated by distinct adhesion molecules. The first step is the initiation of leukocyte rolling along the activated endothelium, a process mainly mediated by the selectins: calcium-dependent low-affinity adhesion molecules consisting of L-selectin (leukocytes), E-selectin (endothelium), and P-selectin (platelets and endothelium) (reviewed by [2]). The second step, firm adhesion and subsequent transmigration of leukocytes into the subendothelium, is mediated primarily by integrins, vascular adhesion molecule-1 (VCAM-1), and intercellular adhesion molecule-1 (ICAM-1).

Although the selectins in general are implicated in initial leukocyte recruitment, studies using P-selectin-deficient mice have shown a key involvement of P-selectin in the development of atherosclerosic lesions. In the absence of P-selectin, both atherosclerotic lesion formation [3–6] and neointimal growth upon arterial injury [7,8] were attenuated in apoE (apoE−/−) and LDL-receptor (LDLR−/−) deficient mice. Studies using immunohistochemistry have shown increased expression of P-selectin protein on the endothelium overlying human atherosclerotic lesions [9], on endothelium of patients with unstable angina [10], and

* Corresponding author. Tel.: +31-71-5276040; fax: +31-71-5276032.
E-mail address: biessen@lacdr.leidenuniv.nl (E.A.L. Biessen).
[1] Members of the UNYPHAR project; a network collaboration between the universities of Groningen, Utrecht, Leiden, and Yamanouchi Europe.

Abbreviations: VCAM, vascular adhesion molecule; ICAM, intercellular adhesion molecule; apoE−/−, apoE deficient mice; WT, wild type; LPS, lipopolysaccharide; sLe^x, sialyl Lewis^x; RT-PCR, reverse transcriptase polymerase chain reaction; P-selectin–IgG, fusion protein of mouse P-selectin and human IgG.

0006-2952/$ – see front matter © 2003 Elsevier Inc. All rights reserved.
doi:10.1016/S0006-2952(03)00387-3

in aortas of hypercholesterolemic rabbits [11,12]. Furthermore, blood-levels of soluble P-selectin, mainly derived from platelets, were found to correlate with the progression of atherosclerosis [13,14], suggesting that platelet P-selectin may be an additional determinant in atherogenesis. However, a quantitative relationship between P-selectin expression and extent of lesion formation in an atherosclerotic animal model has never been shown. Knowledge on the expression pattern of P-selectin throughout all stages of lesion development is essential to evaluate P-selectin as a candidate target in various stages of atherosclerosis.

In the current report, we quantitated the expression of endothelial P-selectin levels in apoE−/− mice by real-time PCR, and compared its tissue specific expression with that of VCAM-1, ICAM-1 and E-selectin. We found that P-selectin mRNA expression correlated with progression of lesion formation, suggesting that P-selectin is a good candidate for intervention, lesion imaging, or targeting strategies. Furthermore, we developed selective P-selectin antagonists by using phage display technology. Such ligands may be useful in the future to identify, target or antagonize P-selectin during atherosclerosis.

2. Materials and methods

2.1. Materials

Mayer's haematoxylin stain, Oil-Red-O, diethylpyrocarbonate, and lipopolysaccharide (type RE 595) were from Sigma. DNAse I (RNAse-free) and glycogen were from Invitrogen. Ribogreen™ was from Molecular Probes. All real-time PCR supplies were from Applied Biosystems. RevertAid™ M-MuLV Reverse Transcriptase was from MBI Fermentas. PCR primers were synthesised by Eurogentec. The pComb8 phage displayed peptide library CX15C (in which X is any amino acid and C is a fixed cystein residue) was generated by Prof. Pannekoek, at the department of Biochemistry, University of Amsterdam. Human P-selectin– and human CD4-IgG were kindly provided by Dr. Appelmelk, Vrije Universiteit. Human E-selectin–IgG was kindly donated by Dr. W. van Dijk, Vrije Universiteit. Mouse P-selectin–IgG and anti-mouse P-selectin antibody wasere from Pharmingen.

2.2. Synthesis of P-selectin binding peptide

Peptides were synthesized according to standard Fmoc solid phase chemistry using an automated peptide synthesizer (9050 Millipore). After cleavage from the resin and simultaneous deprotection in 95% TFA/H_2O, the crude peptides were precipitated by addition of ether and subsequently purified on a C8 RP-column (Alltech) using a acetonitrile/water gradient. Sequence and purity were verified by MALDI/LC–MS. The freeze-dried peptide was stored at −20° under argon until further use. The purity of the peptides was checked by mass spectroscopy and HPLC and was at least 70%.

2.3. Animals

Female apoE−/− and C57bl/6 (control) mice were obtained from Jackson Labs (Bar Harbor) and Broekman (Someren), respectively, and received regular chow. Mice were anaesthetised by subcutaneous injection of ketamine (75 mg/kg; Eurovet), droperidol (1 mg/kg), fluanisone (0.75 mg/kg), and fentanyl (0.04 mg/kg; all from Janssen-Cilag). Following a whole-body 10 min perfusion using ice-cold phosphate-buffered saline, organs were excised, frozen in liquid N_2, and kept at −80° until RNA isolation. The aorta was prepared free of peri-adventitial fat *in situ*. The aortic arch was isolated from the base (most proximal to the heart) and severed from the descending aorta most distal to the left subclavian artery.

2.4. Assessment of lesion formation

Serial sections (10 μm thick) of the aortic arch were cut using a Leica CM3050S cryostat. Ten consecutive sections per mouse were immersed 10 times in 60% isopropanol, incubated for 15 min with Oil-Red-O (0.06% (w/v) in 60% isopropanol), washed and counterstained for 3 min with Mayer's haematoxylin stain. Sections were visualised using a Leica microscope, and lesion area was calculated with Leica imaging software (Qwin).

2.5. Real-time quantitative PCR

Isolated organs and tissues were homogenised and RNA was isolated using Trizol (Boehringer). After removing genomic DNA using RNAse free Dnase I, RNA was reverse transcribed to cDNA using oligo dT primer and SuperScript II RT-polymerase (Pharmacia). mRNA levels were quantitatively determined on an ABI Prism® 7700 Sequence Detection system (Applied Biosystems) using SYBR-green technology. PCR primers (Table 1) were designed using Primer Express 1.5 Software with the manufacturer's default settings (amplicon size: 68–150 base pairs). In 96-well plates, 12.5 μL SYBR-green master was added to 12.5 μL of diluted cDNA (1% of the amount of cDNA derived from 1.0 μg RNA) and 300 nM of forward and reverse primers in water. Expression levels of the cDNA of interest were related to an internal standard: housekeeping gene hypoxanthine phosphoribosyltransferase (HPRT), to correct for differences in quantity and quality between different RNA samples. These levels were analyzed in separate wells. HPRT was used as an internal standard, as it showed constant expression during development of arterial disease, and because expression was also comparable between different organs and tissues (more so than the often-used GAPDH and β-actin levels). Plates were heated for 2 min at 50° and 10 min at 95°.

Table 1
Primer sequences used for real-time PCR

Gene	Accession no.	Primers (forward and reverse, respectively)	Amplicon size
ICAM-1	NM010493	GGACCACGGAGCCAATTTCCTCGGAGACATTAGAGAACAATGC	82
VCAM-1	NM011693	ACAAAACGATCGCTCAAATCGCGCGTTTAGTGGGCTGTCTATC	110
E-sel	NM011345	CCCTGCCCACGGTATCAGCCCTTCCACACAGTCAAACGT	85
P-sel	NM011347	GGTATCCGAAAGATCAACAATAAGTGGTTACTCTTGATGTAGATCTCCACACA	141
HPRT	J00423	TTGCTCGAGATGTCATGAAGGAAGCAGGTCAGCAAAGAACTTATAG	91

Subsequently, 40 PCR cycles consisting of 15 s at 95° and 60 s at 60° were applied. At the end of each run, samples were heated to 95° with a ramp time of 20 min to construct dissociation curves. As SYBR-green only intercalates in double-stranded DNA, melting of the product will result in a sudden decrease in fluorescent signal. From the first-derivative of the fluorescent signal obtained in the dissociation curves, it could be seen that all PCR reactions produced well-defined single PCR products with melting temperatures between 75 and 85°. The absence of genomic DNA contaminations in the RNA preparations was confirmed by running RNA samples that had not been subjected to reverse transcription.

Relative expression levels were determined according to the $\Delta\Delta C_t$ rule (Applied Biosystems, User Bulletin #2). Threshold cycles (C_t) were defined as the number of PCR cycles at which the fluorescent signal reached a fixed threshold signal, being directly proportional to the amount of input. For each combination of target and primers, the ^{10}log of cDNA input was plotted against C_t. The slope of each curve was between −3.3 and −3.5, indicating that PCR amplification efficiencies were close to 100% (efficiency of the PCR is calculated from: efficiency = $10^{[-1/\text{slope}]} - 1$). For each sample, C_ts for the gene of interest and the housekeeping gene HPRT were determined. The ΔC_t ($=C_{t,\text{target gene}} - C_{t,\text{housekeeping gene}}$) was calculated, which is a measure of relative gene expression. The expression levels were related to an external calibrator, that consisted of cDNA from a pool of different mouse organs and tissues (i.e. liver, lung, spleen, heart, and aorta). The external calibrator was included in all determinations. Subsequently, $\Delta\Delta C_t$ ($=\Delta C_{t,\text{sample}} - \Delta C_{t,\text{calibrator}}$) was determined. Relative expression levels, as depicted in Figs. 1 and 2, were then calculated from $2^{-\Delta\Delta C_t}$.

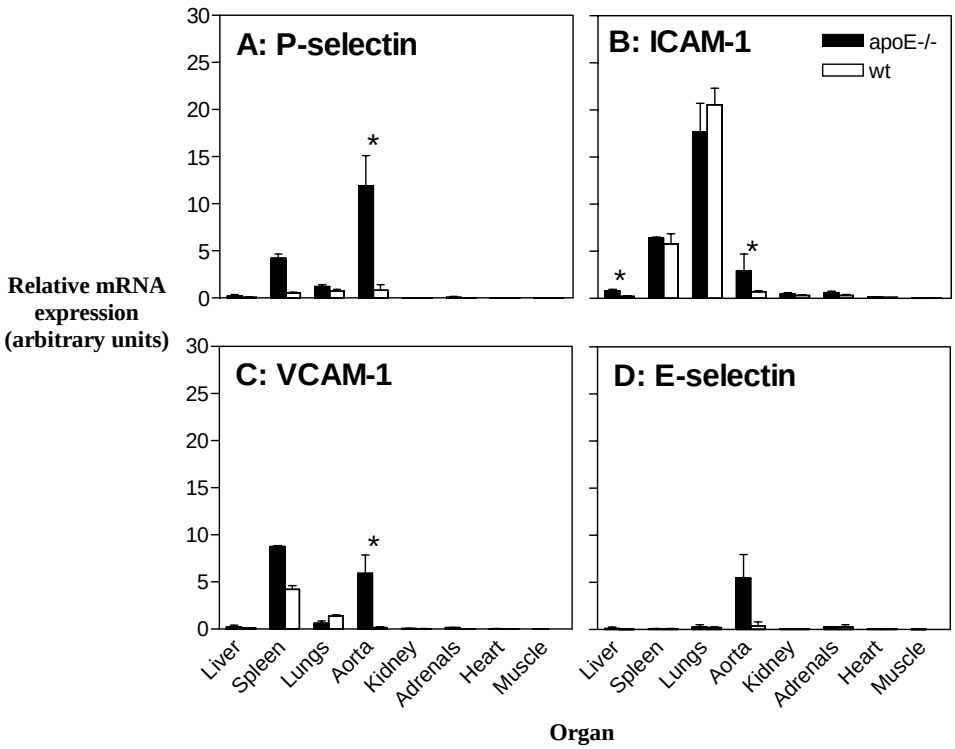

Fig. 1. mRNA levels of various adhesion molecules in organs of apoE-deficient mice. mRNA levels of P-selectin (A), ICAM-1 (B), VCAM-1 (C), and E-selectin (D) were quantified in various organs from 34-week-old apoE−/− and control mice, using real-time PCR technology. Protein expression in apoE−/− mice (black bars) and control mice (white bars) was statistically analyzed by ANOVA, using Tukey–Kramer post-testing. (*) = significantly different ($P < 0.05$). Values represent means of three animals per group ± SD.

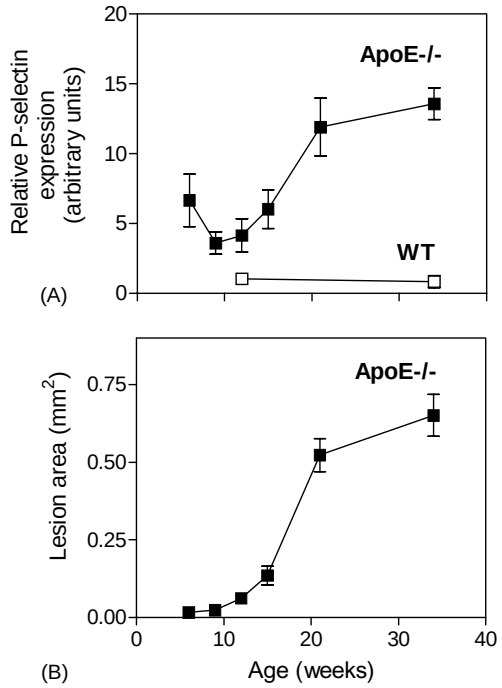

Fig. 2. P-selectin mRNA expression and lesion formation in aortas of 6-, 9-, 12-, 15-, 21-, and 34-week-old apoE-deficient mice. (A) mRNA levels of P-selectin in aortas from apoE-deficient and control mice of different age, quantified using real-time PCR. Values represent means of three animals per group. (B) Lesion size in apoE-deficient mice of different age was determined in 10 serial sections (10 μm) of the aortic arch. Lesions were stained using Oil-Red-O, and quantified with Leica Qwin imaging software. (■) apoE-deficient; (□) wild-type. Values represent means of 5–6 animals per age group ± SD.

2.6. Isolation of P-selectin binding phage

Phage display selections were performed as follows. Fc-specific anti-human IgG was incubated overnight at 4° in a 96 well plate. The next day, wells were washed with assay buffer (20 mM HEPES, 150 mM NaCl, 1 mM $CaCl_2$, pH 7.4), blocked with BSA and incubated with chimeric mouse P-selectin, consisting of the binding domain of mouse P-selectin fused to human IgG (P-selectin–IgG, 0.3 μg/mL) mouse P-selectin–IgG. Wells were incubated for 2 hr with the pComb8 phage library (10^{10} colony forming units). Wells were washed and binding phage were eluted with 0.1 M glycine/HCl, pH 2.2. The isolated phage pool was titered, amplified and purified as described [15]. Amplified phage were used for further selections. DNA sequencing of enriched phage pools was conducted at the DNA-sequencing facility of the Leiden University Medical Center using a standard M13 primer (5′-GACGT-TGTAAAACGACGGCCAGT-3′).

2.7. Competition ELISA

Microtiter wells were coated with mouse P-selectin–IgG as described under Section 2.6. P-selectin coated wells were incubated with HSO_3–Le^a–PAA–biotin (Dextra Laboratories, 0.3 μg/mL in assay buffer containing 0.05% Tween 20 and 0.1% BSA) in the presence of 0–200 μM peptides (2 hr, 37°), washed and incubated with streptavidin-horseradish peroxidase (1:3000 in assay buffer) for 30 min. After washing six times with assay buffer containing 0.1% Tween 20, the wells were incubated for 15 min at RT with 100 μL TMB/H_2O_2 (Pierce). The reaction was stopped by adding 2 M H_2SO_4 and the absorbance read at 450 nm. IC_{50} values were calculated by using the non-linear regression analysis option (variable slope) in GraphPad Prism. Top and bottom of the graphs were held constant at 100 and 0%, respectively.

3. Results

3.1. mRNA expression of adhesion molecules in apoE-deficient mice

We used real-time PCR to evaluate the mRNA expression of P-selectin and other adhesion molecules in aortas of 34-week-old apoE−/− mice fed a regular chow diet. These mice develop lipid-rich fibrocellular lesions with characteristics very similar to those observed in human atherosclerotic lesions [16]. At 34 weeks of age, apoE−/− mice display the entire spectrum of early to advanced lesions over large areas of the aortic tree [17]. The mRNA levels of the adhesion molecules were compared with mRNA levels in other organs and tissues. Their expression was related to the expression level of the housekeeping gene HPRT, which was found to be at a constant level in the tissues of examined apoE−/− and age-matched wild type (WT) animals.

P-selectin was only moderately expressed in lungs, spleen, and aorta of WT animals (Fig. 1A). However, in atherosclerotic aortas from apoE−/− mice, P-selectin expression was strongly increased: a significant 14-fold induction was observed as compared with control mice. In addition, P-selectin mRNA expression had the tendency to be increased in liver (3-fold) and spleen (8-fold), albeit non-significant. P-selectin mRNA expression in other organs such as lungs, adrenals, muscle, heart and kidney of apoE−/− mice did not markedly differ from that in WT tissues (Fig. 1A). As a positive control for systemic inflammation, we treated 12-week-old control mice with lipopolysaccharide (LPS, 100 μg/kg i.v., 5 hr). These animals showed a 130-fold induction in aortic P-selectin expression as compared to untreated mice of the same age (average of N = 5, data not shown).

P-selectin mRNA expression levels were compared with those of other inflammatory adhesion molecules which are suggested to be important in atherogenesis, by measuring mRNA levels of ICAM-1, VCAM-1, and E-selectin in tissues of apoE−/− and WT animals (Fig. 1B, C and D). Moderate- to high basal expression levels of ICAM-1 and VCAM-1 were observed in lungs and spleen of wild type animals. In apoE−/− mice, a significant 4-fold induction

of ICAM-1 mRNA expression was detected in both aorta and liver (Fig. 1B), whereas VCAM-1 expression levels were significantly higher in aorta (38-fold, Fig. 1C). The expression of E-selectin was very low in all WT tissues (Fig. 1D). In apoE−/− mice, E-selectin levels were highly variable between the various mice, but on average there was a tendency towards increased E-selectin levels in the aorta as compared to wild type (16-fold; Fig. 1D).

3.2. Temporal P-selectin mRNA expression and lesion formation

We chose to further assess P-selectin expression, because of its strong induction in atherosclerotic aortic tissue as compared with other tissues (this paper), and because of its reported relevance to atherosclerotic lesion development [3–12]. Vascular mRNA expression level of P-selectin was established at different stages of lesion development in the aortic arch of apoE−/− mice (i.e. 6-, 9-, 12-, 15-, 21- and 34-week-old mice). In Fig. 2A, the P-selectin mRNA expression pattern in the aortic arch is shown in relation to age. Basal P-selectin levels appeared to be induced at all ages as compared with WT animals. Interestingly, P-selectin levels were already increased at 6 weeks, an age at which lesions are not visible. From 9 weeks onwards, P-selectin mRNA expression increased steadily with age, leading upto a 14-fold increase in 34-week-old apoE-deficient mice as compared with age-matched wild-type animals, indicating that the induction of P-selectin expression was not simply due to age-dependent regulation of gene expression.

To match the changes in P-selectin expression to the extent of atherosclerosis, lesion formation was determined at the base of the aortic tree in apoE−/− mice and wild-type mice of increasing age (Fig. 2B). Lesion size at the base of the aortic tree shows a strong, linear correlation with the total aortic lesion area, and is therefore a good measure of the latter [17]. The extent of lesion development was found to correlate well with the P-selectin expression profile (Fig. 2A vs. B). Small fatty-streak areas before 12 weeks of age rapidly progressed into a 8- and 11-fold increased plaque area in 21- and 34-week-old animals, respectively. There were no lesions in aortas from WT animals, regardless of age. Comparable serum total cholesterol levels were found for all age groups of the apoE−/− animals (on average 4.88 ± 0.88 mg/mL, $N = 15$), indicating that the effects on vascular lesion size and P-selectin expression are not attributable to a difference in cholesterol levels (data not shown).

3.3. Screening of a phage displayed peptide library against P-selectin

Based on the above-described findings, we set out to search for P-selectin ligands for use in P-selectin directed imaging of atherosclerotic lesions and for direct

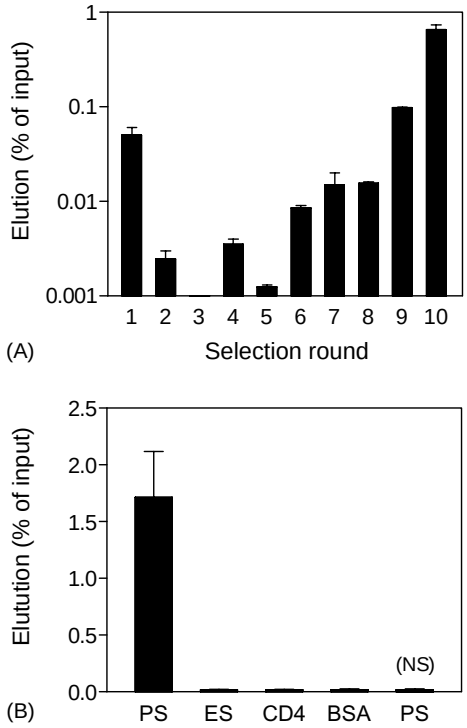

Fig. 3. Isolation of human P-selectin binding phage. (A) Selection on immobilized P-selectin–IgG using the pComb8 phage display peptide library resulted in a 500-fold enrichment of P-selectin binding phage in the 10th round of selection. (B) Phage clone TM33 is specific for P-selectin (PS) as compared to E-selectin (ES), CD4, and bovine serum albumin (BSA). Non-specific phage pools (NS) showed little binding to P-selectin. Values are expressed as the ratio of acid-eluted phage (output) and input titer (approximately 10^9 colony forming) and represent means of triplicate experiments ± SEM.

intervention in P-selectin function. As synthetic drugs (generally sialyl Lewis^x derived glycosides) are inhibitors of P-selectin function with an apparent low affinity for P-selectin [18], we screened a 15 amino acid cystein-constrained phage-displayed peptide library (pComb8-$CX_{15}C$) to identify novel P-selectin binding peptides. For selections, chimeric P-selectin, consisting of human IgG1 fused to the binding domain of mouse P-selectin (P-selectin–IgG), was immobilized onto microtiter wells via an anti-IgG antibody. The biopanning protocol involved a gentle wash in the first round, thus explaining the high relative recovery of binding phage in round 1, and more stringent washes in subsequent/later rounds, which resulted in an approximate 500-fold enrichment of P-selectin binding phage after 10 rounds of biopanning (Fig. 3A). Phage pools from the 9th and 10th selection rounds, containing the P-selectin binding phage, were subjected to DNA sequence analysis to determine the inserted peptide sequence responsible for the enhanced binding. Most of the sequenced phage from the 9th and 10th selection round (42 and 80%, respectively), contained peptide sequence TM33 (Table 2), indicating the importance of this sequence for P-selectin binding. The deletion mutant that was recovered contained no peptide insert, and its presence

Table 2
Peptide sequences found in the 9th and 10th round of selection by screening a CX15C library on mouse P-selectin

Round	Sequence	%	Name
9	CLVSVLDLEPLDAAWLC	42	TM33
	Deletion mutant	21	TM37
10	CLVSVLDLEPLDAAWLC	80	TM33
	Deletion mutant	20	TM37

The percentage indicates their relative occurrence among all sequenced phage in that round.

in later rounds is probably an effect of a growth advantage during phage amplification.

The phage clone displaying peptide TM33 was amplified and purified. Binding of TM33 phage to mouse P-selectin showed a 1000-fold specificity over control proteins (human P-selectin, E-selectin, CD4, BSA; Fig. 3B). TM33 binding to P-selectin was Ca^{2+}-independent, as judged from similar phage recoveries from incubations in the presence of EDTA (data not shown). The binding of phage clone TM33 to P-selectin could be inhibited by a synthetic TM33 peptide (i.e. CLVSVLDLEPLDAAWLC, constrained). At 100 μM TM33 peptide, the recovered amount of TM33 phage was reduced by 75%, indicating that the synthetic peptide itself interacts with P-selectin at the same site as the parent phage clone (Fig. 4A).

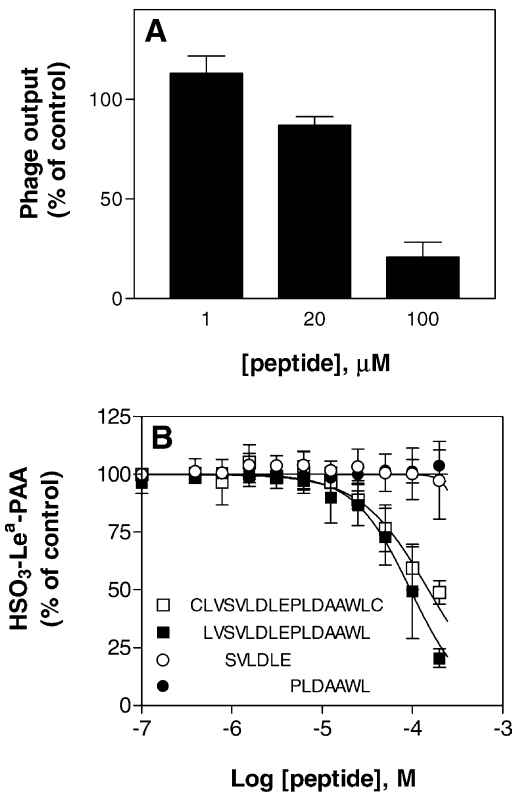

Fig. 4. Displacement of TM33-phage and HSO_3–Le^a binding by synthetic TM33 peptide. (A) Binding of phage clone TM33 (input 10^{10} colony forming units) was determined in the presence of indicated amounts of synthetic TM33 peptide. (B) Competition studies of HSO_3–Le^a–PAA–biotin (0.3 μg/mL) binding to P-selectin by synthetic peptides were performed in an ELISA. (□) CLVSVLDLEPLDAAWLC, IC_{50} = 151 μM; (■) LVSVLDLEPLDAAWL, IC_{50} = 100 μM; (○) SVLDLE; (●) PLDAAWL. Values are expressed as a percentage of total binding phage or HSO_3–Le^a–PAA–biotin binding in the absence of TM33 peptide (=96%), and represent means of triplicate experiments ± SEM.

Competition studies were conducted to investigate whether constrained TM33 was able to inhibit the binding of a natural ligand for P-selectin, sialyl Lewis X (sLe^x) by using the sLe^x analogue sulfated Lewis^a (HSO_3–Le^a), which was conjugated to polyacrilic acid to increase its affinity. As a reference, binding of HSO_3–Le^a–PAA to mouse P-selectin could be completely blocked by an anti-mouse P-selectin antibody (IC_{50} 11 nM, results not shown). Binding of HSO_3–Le^a–PAA binding could was be completely and dose-dependently inhibited by TM33 (Fig. 4B, IC_{50} = 151 μM, 95% confidence interval: 82–112 μM), suggesting that TM33 can be used to antagonize P-selectin function. The linear analogue of TM33, LVSVLDLEPLDAAWL, proved at least equally potent as full-length constrained TM33 (IC_{50} = 96 μM, 95% confidence interval: 123–185 μM), establishing that the terminal cysteins of TM33 and a cyclic configuration are not imperative for P-selectin binding. In contrast, the truncated peptide analogues SVLDLE and PLDAAWL were totally inactive, indicating that the minimal binding motif is not within these short sequences.

4. Discussion

P-selectin is localized in Weibel–Palade bodies of endothelial cells and α-granules of platelets, but is rapidly translocated to the cell surface in response to a variety of inflammatory stimuli such as oxidized lipoproteins, LPS, and thrombin [19,20]. As a result of continuous stimulation, endothelial P-selectin can also be upregulated by enhanced protein synthesis and secretion, which may occur during chronic inflammation [21,22]. Although P-selectin protein is expressed on both human and rabbit atherosclerotic tissue [9,11,12] and has been shown to play a key role in atherogenesis [3–6,23], quantitative information on the expression of P-selectin in an atherosclerotic animal model is lacking. Knowledge of the P-selectin expression pattern is essential to be able to appreciate the potential of P-selectin as a candidate target for diagnostic and/or intervention purposes in atherosclerosis-related disorders.

We assessed the expression pattern of P-selectin in hyperlipidemic apoE−/− mice by using real-time, quantitative RT-PCR, a technique that has also successfully been applied to determine the expression levels of lipoprotein receptors [24], fibroblast growth factor receptor [25], and platelet derived growth factor receptor [26] in atherosclerotic tissues. Although mRNA levels are not necessarily proportional to the production of functional proteins, the correlation between P-selectin mRNA expression and functional protein has been shown in several studies [27,28].

P-selectin expression was significantly induced in atherosclerotic aortas from 34-week-old apoE−/− mice as compared with age-matched controls, which is consistent with enhanced P-selectin protein expression in human and rabbit atherosclerotic endothelium [9,11,12]. The observed increase of ICAM-1, VCAM-1, and E-selectin expression in the aortas of apoE−/− mice confirms the reported induced expression of these adhesion molecules in atherosclerosis [29–31].

We chose to monitor expression of P-selectin in more detail, by correlating expression with progression of lesion development in aortic arch segments from apoE−/− mice. In this atherosclerotic mouse model, lesion development ranges from: (1) enhanced monocyte recruitment to lesion-prone area's of the vascular wall (6–9 weeks of age), (2) formation of early lesions (9–12 weeks of age), to (3) more advanced, complex lesions (12 weeks of age and older) [32,33]. In our study, P-selectin mRNA levels in the aortic arch were remarkably high at 6 weeks. The early appearance of P-selectin in atherosclerosis was also observed by Sakai *et al.* [11]. Probably, prior to lesion formation, P-selectin expression primes the arterial wall, creating a receptive environment for circulating monocytes and greatly reducing their rolling velocity on the arterial surface. After this acute phase of inflammation, P-selectin mRNA expression in aortas of apoE-deficient mice did decrease (9 and 12 weeks), possibly perhaps reflecting the interface between the end of the acute inflammatory phase and the beginning of a more chronic type of inflammation. Between 9 and 34 weeks of age, P-selectin expression correlated well with lesion development (Fig. 2A and B). At this stage, P-selectin protein expression gradually shifts from endothelium covering the lesion site, to the shoulders of more advanced lesions [9]. As new lesions are continuously formed, the age-dependent P-selectin expression probably reflects the vascular surface area that is covered in lesions, rather than local lesion formation. Total vascular P-selectin expression therefore provides a good marker for overall lesion development, implying that strategies to interfere with P-selectin dependent inflammatory responses may have potential at all stages of atherosclerosis. In this respect, its low expression in healthy aortic tissue and other tissues examined, make P-selectin a more suitable target than ICAM-1 and VCAM-1, both showing relatively high levels of expression in large organs such as lung and spleen (Fig. 1A).

The TM33 phage that we identified in this study appeared to specifically bind P-selectin without calcium dependency, and synthetic TM33 peptides were able to displace TM33 phage. Moreover, TM33 peptides inhibited HSO_3–sLe^a binding, suggesting that this 15 amino acid peptide sequence can be used as a lead compound for future intervention studies. We have not yet resolved which part of TM33 is responsible for the interaction with P-selectin. The absence of a consensus sequence hampers the identification of the minimal binding motif of TM33, but truncation and alanine substitution studies may provide further information on the minimal sequence motif and amino acids that are essential for TM33 to interact with P-selectin.

TM33 and derived peptides can serve as a model for testing the potential use of P-selectin binding peptides *in vivo*, using mouse models of atherosclerosis. Likewise, CS-1 peptide, which blocks VLA-4 on the leukocyte surface, was effective in reducing leukocyte recruitment and lipid accumulation in LDLR−/− mice [34]. Small oligopeptides have the advantage that they generally are less immunogenic and more accessible for large-scale synthesis, in contrast to, for example, antibodies. Moreover, radiolabeled peptides can be used in imaging strategies [35]. Our results indicate that aortic P-selectin expression is a valid marker for lesion development, suggesting that P-selectin ligands could be used to image plaque progression *in vivo*. Although the therapeutic use of peptides present some challenges with respect to their pharmacokinetic properties, optimization strategies including the creation of peptidomimetics may provide ways to improve their bioavailability and stability.

This study provides quantitative assessment of P-selectin expression in an atherosclerotic mouse model. P-selectin expression increases with age and is a specific marker for lesion progression more so than the adhesion molecules ICAM-1, VCAM-1, and E-selectin. P-selectin appears to play an important role at all stages of lesion development, and may therefore be a good candidate target for diagnostic purposes and therapeutic interventions in atherosclerosis. Furthermore, the lead structure we have identified in this study may serve as a future P-selectin antagonist or as a useful investigative tool.

Acknowledgments

This project was funded in part by grants 2000D040 and M93.001 from the Netherlands Heart Foundation (JK, EB).

References

[1] Ross R. Atherosclerosis—an inflammatory disease. N Engl J Med 1999;340:115–26.
[2] Vestweber D, Blanks JE. Mechanisms that regulate the function of the selectins and their ligands. Physiol Rev 1999;79:181–213.
[3] Dong ZM, Brown AA, Wagner DD. Prominent role of P-selectin in the development of advanced atherosclerosis in ApoE-deficient mice. Circulation 2000;101:2290–5.
[4] Collins RG, Velji R, Guevara NV, Hicks MJ, Chan L, Beaudet AL. P-selectin or intercellular adhesion molecule (ICAM)-1 deficiency substantially protects against atherosclerosis in apolipoprotein E-deficient mice. J Exp Med 2000;191:189–94.
[5] Johnson RC, et al. Absence of P-selectin delays fatty streak formation in mice. J Clin Invest 1997;99:1037–43.
[6] Nageh MF, Sandberg ET, Marotti KR, Lin AH, Melchior EP, Bullard DC, Beaudet AL. Deficiency of inflammatory cell adhesion molecules

protects against atherosclerosis in mice. Arterioscler Thromb Vasc Biol 1997;17:1517–20.
[7] Kumar A, Hoover JL, Simmons CA, Lindner V, Shebuski RJ. Remodeling and neointimal formation in the carotid artery of normal and P-selectin-deficient mice. Circulation 1997;96:4333–42.
[8] Manka D, Collins RG, Ley K, Beaudet AL, Sarembock IJ. Absence of p-selectin, but not intercellular adhesion molecule-1, attenuates neointimal growth after arterial injury in apolipoprotein e-deficient mice. Circulation 2001;103:1000–5.
[9] Johnson Tidey RR, McGregor JL, Taylor PR, Poston RN. Increase in the adhesion molecule P-selectin in endothelium overlying atherosclerotic plaques. Am J Pathol 1994;144:952–61.
[10] Tenaglia AN, et al. Levels of expression of P-selectin, E-selectin, and intercellular adhesion molecule-1 in coronary atherectomy specimens from patients with stable and unstable angina pectoris. Am J Cardiol 1997;79:742–7.
[11] Sakai A, Kume N, Nishi E, Tanoue K, Miyasaka M, Kita T. P-selectin and vascular cell adhesion molecule-1 are focally expressed in aortas of hypercholesterolemic rabbits before intimal accumulation of macrophages and T lymphocytes. Arterioscler Thromb Vasc Biol 1997;17:310–6.
[12] Gauthier TW, Scalia R, Murohara T, Guo JP, Lefer AM. Nitric oxide protects against leukocyte–endothelium interactions in the early stages of hypercholesterolemia. Arterioscler Thromb Vasc Biol 1995;15:1652–9.
[13] Ridker PM, Buring JE, Rifai N. Soluble P-selectin and the risk of future cardiovascular events. Circulation 2001;103:491–5.
[14] Blann AD, McCollum CN. Increased soluble P-selectin in peripheral artery disease: a new marker for the progression of atherosclerosis. Thromb Haemost 1998;80:1031–2.
[15] Molenaar TJM, Michon I, de Haas SAM, van Berkel TJC, Kuiper J, Biessen EAL. Uptake and processing of modified bacteriophage M13 in mice: implications for phage display. Virology 2002;293:182–91.
[16] Zhang SH, Reddick RL, Piedrahita JA, Maeda N. Spontaneous hypercholesterolemia and arterial lesions in mice lacking apolipoprotein E. Science 1992;258:468–71.
[17] Tangirala RK, Rubin EM, Palinski W. Quantitation of atherosclerosis in murine models: correlation between lesions in the aortic origin and in the entire aorta, and differences in the extent of lesions between sexes in LDL receptor-deficient and apolipoprotein E-deficient mice. J Lipid Res 1995;36:2320–8.
[18] Lefer DJ. Pharmacology of selectin inhibitors in ischemia/reperfusion states. Annu Rev Pharmacol Toxicol 2000;40:283–94.
[19] Vora DK. Induction of P-selectin by oxidized lipoproteins. Separate effects on synthesis and surface expression. Circ Res 1997;80:810–8.
[20] Lorant DE, Patel KD, McIntyre TM, McEver RP, Prescott SM, Zimmerman GA. Coexpression of GMP-140 and PAF by endothelium stimulated by histamine or thrombin: a juxtacrine system for adhesion and activation of neutrophils. J Cell Biol 1991;115:223–34.
[21] Khew Goodall Y. Chronic expression of P-selectin on endothelial cells stimulated by the T-cell cytokine, interleukin-3. Blood 1996;87:1432–8.
[22] Yao L, Pan J, Setiadi H, Patel KD, McEver RP. Interleukin 4 or oncostatin M induces a prolonged increase in P-selectin mRNA and protein in human endothelial cells. J Exp Med 1996;184:81–92.
[23] Ramos CL, Huo Y, Jung U, Ghosh S, Manka DR, Sarembock IJ, Ley K. Direct demonstration of P-selectin- and VCAM-1-dependent mononuclear cell rolling in early atherosclerotic lesions of apolipoprotein E-deficient mice. Circ Res 1999;84:1237–44.
[24] Hiltunen TP, Luoma JS, Nikkari T, Yla Herttuala S. Expression of LDL receptor, VLDL receptor, LDL receptor-related protein, and scavenger receptor in rabbit atherosclerotic lesions: marked induction of scavenger receptor and VLDL receptor expression during lesion development. Circulation 1998;97:1079–86.
[25] Hughes SE. Localisation and differential expression of the fibroblast growth factor receptor (FGFR) multigene family in normal and atherosclerotic human arteries. Cardiovasc Res 1996;32:557–69.
[26] Krettek A, Fager G, Jernberg P, Ostergren Lunden G, Lustig F. Quantitation of platelet-derived growth factor receptors in human arterial smooth muscle cells *in vitro*. Arterioscler Thromb Vasc Biol 1997;17:2395–404.
[27] Armstead VE, Minchenko AG, Schuhl RA, Hayward R, Nossuli TO, Lefer AM. Regulation of P-selectin expression in human endothelial cells by nitric oxide. Am J Physiol 1997;273:740–6.
[28] Eguchi H, Ikeda H, Murohara T, Yasukawa H, Haramaki N, Sakisaka S, Imaizumi T. Endothelial injuries of coronary arteries distal to thrombotic sites: role of adhesive interaction between endothelial P-selectin and leukocyte sialyl LewisX. Circ Res 1999;84:525–35.
[29] Kd OB, McDonald TO, Chait A, Allen MD, Alpers CE. Neovascular expression of E-selectin, intercellular adhesion molecule-1, and vascular cell adhesion molecule-1 in human atherosclerosis and their relation to intimal leukocyte content. Circulation 1996;93:672–82.
[30] van der Wal AC, Das PK, Tigges AJ, Becker AE. Adhesion molecules on the endothelium and mononuclear cells in human atherosclerotic lesions. Am J Pathol 1992;141:1427–33.
[31] Nakashima Y, Raines EW, Plump AS, Breslow JL, Ross R. Upregulation of VCAM-1 and ICAM-1 at atherosclerosis-prone sites on the endothelium in the ApoE-deficient mouse. Arterioscler Thromb Vasc Biol 1998;18:842–51.
[32] Nakashima Y, Plump AS, Raines EW, Breslow JL, Ross R. ApoE-deficient mice develop lesions of all phases of atherosclerosis throughout the arterial tree. Arterioscler Thromb 1994;14:133–40.
[33] Reddick RL, Zhang SH, Maeda N. Atherosclerosis in mice lacking apo E. Evaluation of lesional development and progression. Arterioscler Thromb 1994;14:141–7.
[34] Shih PT, Brennan ML, Vora DK, Territo MC, Strahl D, Elices MJ, Lusis AJ, Berliner JA. Blocking very late antigen-4 integrin decreases leukocyte entry and fatty streak formation in mice fed an atherogenic diet. Circ Res 1999;84:345–51.
[35] Welling MM, Nibbering PH, Paulusma Annema A, Hiemstra PS, Pauwels EK, Calame W. Imaging of bacterial infections with 99mTc-labeled human neutrophil peptide. J Nucl Med 1999;40:2073–80.